ISSN (Print) : 2320 – 3765
ISSN (Online): 2278 – 8875

International Journal of Advanced Research in Electrical, Electronics and Instrumentation Engineering

(A High Impact Factor, Monthly, Peer Reviewed Journal)

Website: www.ijareeie.com

Vol. 8, Issue 8, August 2019

Observer and Fuzzy Neural Network based 3-Axis MEMS Gyroscope Nonlinear Control

Olivier Baraka Mushage

Associate Professor, Faculty of Applied Sciences and Technologies, Dept. of Electrical and Computer Engineering,

Université Libre des Pays des Grands Lacs, Goma, DRC

ABSTRACT: In this paper, a nonlinear controller has been presented for a 3-axis Micro-Electro-Mechanical System (MEMS) gyroscope subject to uncertain parameters or dynamics and external disturbances. Considering that some state variables may be unavailable for the controller's operation, a model-free high-gain state observer is used to generate an estimation of the state vector. The controller uses an approximation of the MEMS dynamics provided by a Fuzzy Neural Network (FNN) by exploiting its universal approximation theorem. The nonlinear control law uses some dynamic parameters tuned online to cancel the adverse effects of external disturbances and FNN approximation errors. Update rules for these parameters and the FNN weights are designed. A stability analysis is performed, using the Lyapunov's method, to prove the stability of the closed-loop system with the proposed control scheme. Numerical simulation results obtained using MATLAB/SIMULINK are presented to demonstrate the good performance of the 3-axis MEMS gyroscope controller.

KEYWORDS: Nonlinear control, MEMS, gyroscope, state observer, fuzzy neural network.

I. INTRODUCTION

Thanks to the fast development of micro and nanotechnologies, Micro-Electro-Mechanical System (MEMS) gyroscopes are being widely considered in control and measurement systems for their small size, low cost, and low power consumption [1-5]. MEMS gyroscopes are used for angular velocity measurement in a wide range of applications in different fields like aerospace, aviation, navigation (GPS-assisted inertial navigation), biotechnology, automotive (stability control and GPS), medicine, consumer electronics (camera image stabilization and 3-D mouse), etc. [2, 6-8]. MEMS gyroscopes pose unique measurement and control problems due to their small size, low cost and low power consumption [1]. In many applications of MEMS gyroscopes, accuracy is required in the tracking of a chosen reference trajectory despite fabrication imperfections, unknown time varying parameters, non-measurable state variables and external disturbances.

In order to ensure good performances for MEMS gyroscopes, despite the aforementioned perturbations, multiple robust and adaptive control algorithms have been proposed. Many of these control schemes use intelligent systems like fuzzy logic systems for their very good ability of approximating unknown dynamics [2, 3].

An adaptive fuzzy sliding mode sliding mode controller has been developed in [4] for MEMS triaxial gyroscopes subject to uncertain dynamics and external disturbances. The proposed controller uses an adaptive identification scheme combined with sliding mode control (SMC), which can identify angular velocity along with other system parameters. Upper and lower bounds of uncertainties and external disturbances are approximated based on Lyapunov methods.

An adaptive fuzzy control approach for electrostatically actuated MEMS subject to uncertain dynamics and unavailable state measurements has been proposed in [5]. The authors used differential theory and output feedback for the controller's design. A fuzzy neural network (FNN) was used to find an approximation of the unknown dynamics. A state observer was used to estimate the state vector needed for the controller's operation.

The control problem of micro-gyroscope systems has been addressed in [6] by considering fabrication imperfections, time varying system parameters, and external disturbances. The authors proposed an adaptive fuzzy SMC, which synchronously tackles the aforementioned issues.

Authors of [7] have proposed an adaptive controller for MEMS gyroscope by combining dynamic surface control, SMC and fuzzy logic. This fuzzy system has been used to approximate the dynamic characteristics of the gyroscope, while the SMC was used to compensate fuzzy approximation error.

ISSN (Print) : 2320 – 3765
ISSN (Online): 2278 – 8875

International Journal of Advanced Research in Electrical, Electronics and Instrumentation Engineering

(A High Impact Factor, Monthly, Peer Reviewed Journal)

Website: www.ijareeie.com

Vol. 8, Issue 8, August 2019

An adaptive fuzzy terminal SMC has been introduced in [8] for the MEMS gyroscope by considering the presence of external disturbances and model uncertainties. The scheme uses an extended Kalman filter to estimate nonlinear dynamics affected by noise.

Authors of [9] have proposed a MEMS gyroscope adaptive global sliding mode fuzzy controller using radial basis function neural network (RBFNN) and the backstepping technique. The RBFNN is used to approximate the unknown dynamics, while the fuzzy controller is used to suppress the chattering phenomenon related to SMC.

In order to deal with state measurement issues, a backstepping controller with an adaptive neural states observer was proposed in [10] for MEMS gyroscopes subject to external disturbances and model uncertainties.

In this paper, an adaptive controller is proposed, which combines a FNN, a nonlinear control scheme and a model-free state observer. The key contribution of this paper is that, unlike for the aforementioned published works, which mostly focus on 2-axis MEMS gyroscopes, a new nonlinear control algorithm is developed for a MEMS gyroscope capable of sensing angular motion about three axes simultaneously (3-axis MEMS gyroscope). The proposed scheme is able to tackle simultaneously issues related to unavailable full state measurement, external disturbances and uncertain system parameters. Considering the unavailability of the system's dynamics, a model-free high gain state observer is designed and used to provide an accurate estimate of the MEMS state vector. A FNN is used to provide an approximation of the unknown dynamics to be used in a nonlinear adaptive control scheme. Time varying parameters are incorporated in the design such that they are adjusted online to compensate the adverse effects of external disturbances and FNN approximation errors. This is important as no prior knowledge of upper bounds for these perturbations is needed, unlike for other control schemes where this requirement has been undermined (see for instance in [1, 6-8, 11] and references therein). The learning rule for the FNN and the adaptive parameters are derived using Lyapunov's methods. Another important contribution is that the proposed controller guarantees very good tracking accuracy.

This paper is organized as follows: Section II gives the model of a 3-axis MEMS gyroscope and states the control problem. In section III the FNN and observer-based nonlinear control strategy is presented and a stability analysis is provided. Numerical simulation results are presented in section IV and finally the paper ends with a conclusion.

II. PROBLEM STATEMENT

A typical MEMS gyroscope is made of a proof mass suspended to a rigid frame by springs and dampers, a sensing mechanism and an electrostatic actuation for forcing an oscillatory motion.

By considering that the gyroscope is moving at a constant linear speed and rotating at a constant angular velocity, and by assuming that centrifugal forces are negligible because of small displacement, the dynamics of a MEMS gyroscope undergoing rotations along x, y and z axis is as follows [4]:

$$\begin{aligned}
m\ddot{x} + d_{xx}\dot{x} + d_{xy}\dot{y} + d_{xz}\dot{z} + k_{xx}x + k_{xy}y + k_{xz}z &= u_x + 2m\Omega_z\dot{y} - 2m\Omega_y\dot{z} \\
m\ddot{y} + d_{xy}\dot{x} + d_{yy}\dot{y} + d_{yz}\dot{z} + k_{xy}x + k_{yy}y + k_{yz}z &= u_y + 2m\Omega_x\dot{z} - 2m\Omega_z\dot{x} \\
m\ddot{z} + d_{xz}\dot{x} + d_{yz}\dot{y} + d_{zz}\dot{z} + k_{xz}x + k_{yz}y + k_{zz}z &= u_z + 2m\Omega_y\dot{x} - 2m\Omega_x\dot{y}
\end{aligned} \tag{1}$$

where m is the mass of proof mass, which can be known exactly; x, y and z are the coordinates of the proof mass with respect to the gyro frame in a Cartesian coordinate system; k_{xy}, k_{xz} and k_{yz} are asymmetric spring stiffness terms due to fabrication imperfections; d_{xy}, d_{xz} and d_{yz} are asymmetric damping factors due to fabrication imperfections; k_{xx}, k_{yy} and k_{zz} are the spring stiffness terms in the x, y and z direction, respectively; d_{xx}, d_{yy} and d_{zz} are the damping factors in the x, y and z direction, respectively; Ω_x, Ω_y and Ω_z are the angular velocities in the x, y and z direction, respectively; u_x, u_y and u_z are the control forces in the x, y and z direction, respectively.

Let us divide Eq. (1) by m and rewrite it as follows:

$$\ddot{\boldsymbol{q}} + \frac{\boldsymbol{D}}{m}\dot{\boldsymbol{q}} + \frac{\boldsymbol{K_a}}{m}\boldsymbol{q} = \frac{\boldsymbol{u}}{m} - 2\boldsymbol{\Omega}\dot{\boldsymbol{q}} \tag{2}$$

where $\boldsymbol{q} = [x \quad y \quad z]^T$, $\boldsymbol{u} = [u_x \quad u_y \quad u_z]^T$, $\boldsymbol{D} = \begin{bmatrix} d_{xx} & d_{xy} & d_{xz} \\ d_{xy} & d_{yy} & d_{yz} \\ d_{xz} & d_{yz} & d_{zz} \end{bmatrix}$, $\boldsymbol{K_a} = \begin{bmatrix} k_{xx} & k_{xy} & k_{xz} \\ k_{xy} & k_{yy} & k_{yz} \\ k_{xz} & k_{yz} & k_{zz} \end{bmatrix}$ and

ISSN (Print) : 2320 – 3765
ISSN (Online): 2278 – 8875

International Journal of Advanced Research in Electrical, Electronics and Instrumentation Engineering

(A High Impact Factor, Monthly, Peer Reviewed Journal)

Website: www.ijareeie.com

Vol. 8, Issue 8, August 2019

$\boldsymbol{\Omega} = \begin{bmatrix} 0 & -\Omega_z & \Omega_y \\ \Omega_z & 0 & -\Omega_x \\ -\Omega_y & \Omega_x & 0 \end{bmatrix}$. Using non-dimensional time $t^* = \omega_0 t$ and dividing both sides of Eq. (2) by m, q_0 (reference length) and ω_0 (natural resonance frequency) yields the non-dimensional equation of motion as follows:

$$\frac{\ddot{\boldsymbol{q}}}{\boldsymbol{q_0}} + \frac{\boldsymbol{D}}{\boldsymbol{m\omega_0}}\frac{\dot{\boldsymbol{q}}}{\boldsymbol{q_0}} + \frac{\boldsymbol{K_a}}{\boldsymbol{m\omega_0^2}}\frac{\boldsymbol{q}}{\boldsymbol{q_0}} = \frac{\boldsymbol{u}}{\boldsymbol{m\omega_0^2 q_0}} - 2\frac{\boldsymbol{\Omega}}{\boldsymbol{\omega_0}}\frac{\dot{\boldsymbol{q}}}{\boldsymbol{q_0}} \quad (3)$$

Let us define a set of new variables as follows:

$q^* = q/q_0,\ D^* = \frac{D}{m\omega_0},\ \Omega^* = \frac{\Omega}{\omega_0},\ u^* = \frac{u}{m\omega_0^2 q_0},\ \omega_x = \sqrt{\frac{k_{xx}}{m\omega_0^2}},\ \omega_y = \sqrt{\frac{k_{yy}}{m\omega_0^2}},\ \omega_z = \sqrt{\frac{k_{zz}}{m\omega_0^2}},\ \omega_{xy} = \frac{k_{xy}}{m\omega_0^2},$
$\omega_{yz} = \frac{k_{yz}}{m\omega_0^2},\ \omega_{xz} = \frac{k_{xz}}{m\omega_0^2}.$

These new variables are used in Eq. (3). For the sake of clarity, let us ignore the superscript $(*)$ and rewrite the non-dimensional equation of motion as follows:

$$\ddot{\boldsymbol{q}} + \boldsymbol{D}\dot{\boldsymbol{q}} + \boldsymbol{K_b q} = \boldsymbol{u} - \boldsymbol{2\Omega}\dot{\boldsymbol{q}} - \boldsymbol{d}(t) \quad (4)$$

where $\boldsymbol{K_b} = \begin{bmatrix} \omega_x^2 & \omega_{xy} & \omega_{xz} \\ \omega_{xy} & \omega_y^2 & \omega_{yz} \\ \omega_{xz} & \omega_{yz} & \omega_z^2 \end{bmatrix}$ and $\boldsymbol{d}(t) = [d_1(t) \quad d_2(t) \quad d_3(t)]^T$ is the vector of external disturbances.

Remark 1: It is considered that the MEMS gyroscope parameters D, K_b and Ω are unknown, the velocity vector $\dot{q}$ measurement is unavailable, and the external disturbances $d(t)$ are unknown.

The objective for the MEMS gyroscope is to maintain the proof mass oscillating in x, y and z directions at frequencies ω_1, ω_2 and ω_3 and at amplitudes X_m, Y_m and Z_m, respectively. This desired trajectory can be stated as $\boldsymbol{q_m} = [x_m \quad y_m \quad z_m]^T$, $x_m = X_m \sin(\omega_1 t)$, $y_m = Y_m \sin(\omega_2 t)$ and $z_m = Z_m, \sin(\omega_3 t)$. The objective is to design a controller that will provide $\boldsymbol{u} \epsilon \mathbb{R}^3$ to ensure the system's state vector $\boldsymbol{q}(t)$ tracks the desired state $q_m(t)$ with accuracy despite the external disturbances $\boldsymbol{d}(t)$, the unavailable velocity $\dot{\boldsymbol{q}}$ measurements and the unknown system parameters ($\boldsymbol{D}$, $\boldsymbol{K_b}$ and $\boldsymbol{\Omega}$).

III. OBSERVER AND FNN BASED NONLINEAR CONTROLLER DESIGN

III.1. HIGH GAIN STATE OBSERVER DESIGN

As stated in Remark 1, the position vector $\boldsymbol{q}$ is available while the velocity vector $\dot{\boldsymbol{q}}$ is unavailable. These two vectors are essential for the controller's operation. In this paper, we choose to use a high-gain state observer that will provide an accurate estimate $\dot{\hat{\boldsymbol{q}}} = [\dot{\hat{\boldsymbol{x}}} \quad \dot{\hat{\boldsymbol{y}}} \quad \dot{\hat{\boldsymbol{z}}}]^{\boldsymbol{T}}$ of the velocity vector.
Let us rewrite Eq. (4) in its state-space form as follows:

$$\begin{cases} \dot{\boldsymbol{X}} = \boldsymbol{AX} + \boldsymbol{f}(\boldsymbol{X}, \boldsymbol{u}) \\ \boldsymbol{Y} = \boldsymbol{CX} \end{cases} \quad (5)$$

where $\boldsymbol{X^T} = [\boldsymbol{X_1} \quad \boldsymbol{X_2} \quad \boldsymbol{X_3}]$ is the state vector with $\boldsymbol{X_1} = [x \quad \dot{x}]^T$, $\boldsymbol{X_2} = [y \quad \dot{y}]^T$ and $\boldsymbol{X_3} = [z \quad \dot{z}]^T$; $\boldsymbol{Y} = [x \quad y \quad z]^T$ is the system's output vector.

$$\boldsymbol{f}(\boldsymbol{X}, \boldsymbol{u}) = -\boldsymbol{B}[(\boldsymbol{D} + \boldsymbol{2\Omega})\dot{\boldsymbol{q}} + \boldsymbol{K_b q} - \boldsymbol{d}(\boldsymbol{t}) - \boldsymbol{u}] \quad (6)$$

ISSN (Print) : 2320 – 3765
ISSN (Online): 2278 – 8875

International Journal of Advanced Research in Electrical, Electronics and Instrumentation Engineering

(A High Impact Factor, Monthly, Peer Reviewed Journal)

Website: www.ijareeie.com

Vol. 8, Issue 8, August 2019

For $i = 1,2,3$ $\boldsymbol{A} = \mathbf{diag}[\boldsymbol{A_1} \quad \boldsymbol{A_2} \quad \boldsymbol{A_3}]$ with $\boldsymbol{A_i} = \begin{bmatrix} 0 & 1 \\ 0 & 0 \end{bmatrix}$, $\boldsymbol{B} = \mathbf{diag}[\boldsymbol{B_1} \quad \boldsymbol{B_2} \quad \boldsymbol{B_3}]$ with $\boldsymbol{B} = \begin{bmatrix} \mathbf{0} \\ \mathbf{1} \end{bmatrix}$, and $\boldsymbol{C} = \mathbf{diag}[\boldsymbol{C_1} \quad \boldsymbol{C_2} \quad \boldsymbol{C_3}]$ with $\boldsymbol{C_i} = [1 \quad 0]$ such that $\boldsymbol{N} = [\boldsymbol{C^T}\!: \quad \boldsymbol{A^T C^T}\!: \quad (\boldsymbol{A^T})^2\boldsymbol{C^T}\!: \quad (\boldsymbol{A^T})^3\boldsymbol{C^T}\!: \quad (\boldsymbol{A^T})^4\boldsymbol{C^T}\!: \quad (\boldsymbol{A^T})^5\boldsymbol{C^T}\!:]$ is a full rank matrix; therefore the system is fully observable.

Assumption 1 [18-23]: The nonlinear vector field $\boldsymbol{f}(\boldsymbol{X},\boldsymbol{u})$ is bounded with respect to its arguments on a compact set $\Delta \subset \mathbb{R}^3$ over which the state vector $X \in \mathbb{R}^6$ is bounded and the control action $\boldsymbol{u} \in \mathbb{R}^3$ is restricted to the class of admissible control forces $\boldsymbol{U} \in \mathbb{R}^3$; therefore, there exist a positive scalar valued function $\boldsymbol{\rho}(\boldsymbol{X},\boldsymbol{u})$ such that $\|\boldsymbol{f}(\boldsymbol{X},\boldsymbol{u})\| \le \|\boldsymbol{P}\|^{-1}\boldsymbol{\rho}(\boldsymbol{X},\boldsymbol{u})$ $\forall \boldsymbol{X} \in \mathbb{R}^6$ and $\forall \boldsymbol{u} \in \mathbb{R}^3$, with $\boldsymbol{P} = \boldsymbol{P^T} > \mathbf{0}$.

In order to design the state observer, we must consider the fact that the system's dynamics is not available and that the only available information is the position vector $\boldsymbol{q}$. Thus, this must be a model-free observer that does not involve the MEMS dynamics in its implementation and for which the input is the MEMS output vector $\boldsymbol{y}$. Let us design the observer such that its state vector $\widehat{\boldsymbol{X}}$ will converge asymptotically towards $\boldsymbol{X}$, i.e. $\lim_{t\to\infty}(\widehat{\boldsymbol{X}} - \boldsymbol{X}) = 0$. We use a model-free high-gain state observer modelled as follows:

$$\begin{cases} \dot{\widehat{\boldsymbol{X}}} = \boldsymbol{A}\boldsymbol{X} + \boldsymbol{L}(\boldsymbol{Y} - \widehat{\boldsymbol{Y}}) \\ \widehat{\boldsymbol{Y}} = \boldsymbol{C}\widehat{\boldsymbol{X}} \end{cases} \tag{7}$$

with $\boldsymbol{L} = \mathbf{block-diag}[\boldsymbol{L_1} \quad \boldsymbol{L_2} \quad \boldsymbol{L_3}]$ being the time-varying high-gain observer matrix where $\boldsymbol{L_i^T} = [k_{i,1}/\sigma(t) \quad k_{i,2}/\sigma^2(t)]$ for which $k_{i,1}$ and $k_{i,2}$ have to be chosen such that the polynomial $p^2 + k_{i,1}p + k_{i,1} = 0$ is Hurwitz and the time varying parameter $\sigma(t) \in \mathbb{R}^+$ is selected as follows [12]:

$$\sigma(t) = \frac{1+\exp(-50t)}{800[1-\exp(-50t)]} \tag{8}$$

Defining the state estimation error as $\widetilde{\boldsymbol{X}} = \boldsymbol{X} - \widehat{\boldsymbol{X}}$ and using Eqs. (5) and (7) we obtain:

$$\begin{aligned} \dot{\widetilde{\boldsymbol{X}}} &= \boldsymbol{X} - \dot{\widehat{\boldsymbol{X}}} \\ &= \boldsymbol{A_0}\widetilde{\boldsymbol{X}} + \boldsymbol{f}(\boldsymbol{X},\boldsymbol{u}) \end{aligned} \tag{9}$$

where the matrix $\boldsymbol{A_0} = (\boldsymbol{A} - \boldsymbol{LC})$ has all its Eigen values with negative real parts.

To check the convergence property of the high-gain state observer, let us use the following candidate Lyapunov's function:

$$V = \frac{1}{2}\widetilde{\boldsymbol{X}}^{\boldsymbol{T}}\boldsymbol{P}\widetilde{\boldsymbol{X}} \tag{10}$$

where $\boldsymbol{P} = \boldsymbol{P^T} > \mathbf{0} \in \mathbb{R}^{6\times6}$ is the solution of the Riccati algebraic equation given as follows:

$$\boldsymbol{A_0^T}\boldsymbol{P} + \boldsymbol{P}\boldsymbol{A_0} = -\boldsymbol{Q} \tag{11}$$

for a given value of $\boldsymbol{Q} = \boldsymbol{Q^T} > \mathbf{0} \in \mathbb{R}^{6\times6}$. Considering assumption 1and Eq. (10) in the derivative of the Lyapunov's function with respect to time we obtain

$$\begin{aligned} \dot{V} &= \frac{1}{2}\dot{\widetilde{\boldsymbol{X}}}^{\boldsymbol{T}}\boldsymbol{P}\widetilde{\boldsymbol{X}} + \frac{1}{2}\widetilde{\boldsymbol{X}}^{\boldsymbol{T}}\boldsymbol{P}\dot{\widetilde{\boldsymbol{X}}} \\ &= \frac{1}{2}\widetilde{\boldsymbol{X}}^{\boldsymbol{T}}(\boldsymbol{A_0^T}\boldsymbol{P} + \boldsymbol{P}\boldsymbol{A_0})\widetilde{\boldsymbol{X}} + \widetilde{\boldsymbol{X}}^{\boldsymbol{T}}\boldsymbol{P}\boldsymbol{f}(\boldsymbol{X},\boldsymbol{u}) \\ &= -\frac{1}{2}\widetilde{\boldsymbol{X}}^{\boldsymbol{T}}\boldsymbol{Q}\widetilde{\boldsymbol{X}} + \widetilde{\boldsymbol{X}}^{\boldsymbol{T}}\boldsymbol{P}\boldsymbol{f}(\boldsymbol{X},\boldsymbol{u}) \\ &\le -\frac{1}{2}\widetilde{\boldsymbol{X}}^{\boldsymbol{T}}\boldsymbol{Q}\widetilde{\boldsymbol{X}} + \|\widetilde{\boldsymbol{X}}\|\|\boldsymbol{P}\|\|\boldsymbol{f}(\boldsymbol{X},\boldsymbol{u})\| \end{aligned} \tag{12}$$

ISSN (Print) : 2320 – 3765
ISSN (Online): 2278 – 8875

International Journal of Advanced Research in Electrical, Electronics and Instrumentation Engineering

(A High Impact Factor, Monthly, Peer Reviewed Journal)

Website: www.ijareeie.com

Vol. 8, Issue 8, August 2019

$$\le -\frac{1}{2}\widetilde{\boldsymbol{X}}^{\boldsymbol{T}}\boldsymbol{Q}\widetilde{\boldsymbol{X}} + \|\widetilde{\boldsymbol{X}}\|\rho(X,u)$$
$$\le -\frac{1}{2}\lambda_{min}(\boldsymbol{Q})\|\widetilde{\boldsymbol{X}}\|^2 + \|\widetilde{\boldsymbol{X}}\|\rho(X,u)$$

where $\lambda_{min}(\boldsymbol{Q})$ is the smallest eigenvalue of $\boldsymbol{Q}$. Thus, whenever $\|\widetilde{\boldsymbol{X}}\|$ is outside the region bounded by $\|\widetilde{\boldsymbol{X}}\| \le 2\rho(\boldsymbol{X},\boldsymbol{u})/\lambda_{min}(\boldsymbol{Q})$ we have $\dot{V} \le 0$. Hence, according to Barbalat's lemma, $\forall t \ge 0$, $\lim_{t\to\infty}(\boldsymbol{X} - \widehat{\boldsymbol{X}}) = 0$, which mean that the observer has a good convergence property, and that $\widehat{\boldsymbol{X}}$ is guaranteed to be bounded in the compact set Δ. This good convergence property is illustrated in Fig. 2 (given in section IV).

III.2. CONTROLLER DESIGN

Let us recall that in this paper we consider that the 3-axis MEMS gyroscope's parameters are unknown; hence the vector function given by:

$$\boldsymbol{f}(\boldsymbol{q},\dot{\boldsymbol{q}}) = [(\boldsymbol{D} + 2\boldsymbol{\Omega})\dot{\boldsymbol{q}} + \boldsymbol{K_b}\boldsymbol{q}] \tag{13}$$

is unknown, while it may be required for the controller's good operation. It is worth mentioning that the external disturbance's vector $\boldsymbol{d}(\boldsymbol{t})$ upper bound is unknown as well. As full state measurement is unavailable, the high-gain observer states $(\widehat{\boldsymbol{q}},\dot{\widehat{\boldsymbol{q}}})$ will be used for the controller's operation.

To deal with the unknown dynamics issue, let us approximate the vector function of the approximate state vector, i.e. $\boldsymbol{f}(\widehat{\boldsymbol{q}},\dot{\widehat{\boldsymbol{q}}})$**.** Considering that the state vector $\widehat{\boldsymbol{X}}$ remains bounded over the compact set $\Delta\in \mathbb{R}^6$ for all $t > 0$, we exploit the universal approximation theorem related to FNN. It has been shown in the literature that FNN are able to approximate any function defined on a compact set Δ to arbitrary accuracy [11, 16, 18].

Thanks to a FNN using a center-of-gravity defuzzification method, the approximation of the vector function can be computed as $\widehat{\boldsymbol{f}}(\widehat{\boldsymbol{q}},\dot{\widehat{\boldsymbol{q}}}) = [\boldsymbol{f_1} \quad \boldsymbol{f_2} \quad \boldsymbol{f_3}]^T$ where, for $i = 1, 2, 3$, we have:

$$\hat{f}_i(\boldsymbol{X_{ei}}|\widehat{\boldsymbol{\theta}}_{\boldsymbol{i}}) = \frac{\sum_{j=1}^{n}\hat{\theta}_{i,j}(t)\left(\prod_{l=1}^{k}\mu_{A_l^j}(X_{ei,l})\right)}{\sum_{j=1}^{n}\left(\prod_{l=1}^{k}\mu_{A_l^j}(X_{ei,l})\right)} = \hat{\theta}_i^T(t)\varphi(\boldsymbol{X_{ei}}) \tag{14}$$

In Eq. (14), n is the number of fuzzy rules, k is the length of the FNN's ith input vector $\boldsymbol{X_{ei}}$ defined in this paper as $\boldsymbol{X_{e1}} = [x_m - \hat{x} \quad \dot{x}_m - \dot{\hat{x}}]$, $\boldsymbol{X_{e2}} = [y_m - \hat{y} \quad \dot{y}_m - \dot{\hat{y}}]$ and $\boldsymbol{X_{e3}} = [z_m - \hat{z} \quad \dot{z}_m - \dot{\hat{z}}]$ for the x-axis, the y-axis and the z-axis, respectively. The FNN weighting vector for the ith axis is $\widehat{\boldsymbol{\theta}}_{\boldsymbol{i}}^{\boldsymbol{T}}(t) = [\hat{\theta}_{i1} \quad \cdots \quad \hat{\theta}_{in}]$. $\varphi(\boldsymbol{X_{ei}}) \in \mathbb{R}^n$ is the fuzzy basis function vector for the ith axis, for which the components $\varphi_j(\boldsymbol{X_{ei}})$ are obtained as follows

$$\varphi_j(\boldsymbol{X_{ei}}) = \frac{\prod_{l=1}^{k}\mu_{A_l^j}(X_{ei,l})}{\sum_{j=1}^{n}\left(\prod_{l=1}^{k}\mu_{A_l^j}(X_{ei,l})\right)} \tag{15}$$

for $1 \le j \le n$, where A_l^j are fuzzy sets corresponding to the membership functions $\mu_{A_l^j}$, for $1 \le l \le k$ and $1 \le l \le n$, computed for each input $X_{ei,l}$ using the following Gaussian function:

$$\mu_{A_l^j}(X_{ei,l}) = \exp\left[-\frac{\left(X_{ei,l} - a_{i,l}^j\right)^2}{2\mu^2}\right] \tag{16}$$

ISSN (Print) : 2320 – 3765
ISSN (Online): 2278 – 8875

International Journal of Advanced Research in Electrical, Electronics and Instrumentation Engineering

(A High Impact Factor, Monthly, Peer Reviewed Journal)

Website: www.ijareeie.com

Vol. 8, Issue 8, August 2019

where $a_{i,l}^{j}$ is the width of the Gaussian function and $\mu > 0$ is the center of the receptive field. These parameters, known as membership function parameter set, and the number of fuzzy rules (n) are very relevant for the accuracy of the FNN output. The approximate vector function at the FNN's output can therefore be written as follows:

$$\hat{\boldsymbol{f}}(\boldsymbol{X}_e|\hat{\boldsymbol{\theta}}) = \hat{\boldsymbol{\theta}}^{\boldsymbol{T}}\boldsymbol{\varphi}(\boldsymbol{X}_e) \quad (17)$$

where $\boldsymbol{\varphi}^T(\boldsymbol{X}_e) = [\varphi^T(\boldsymbol{X}_{e,1}) \quad \varphi^T(\boldsymbol{X}_{e,2}) \quad \varphi^T(\boldsymbol{X}_{e,3})] \in \mathbb{R}^{\boldsymbol{3n}}$ is the vector of radial basis functions and $\hat{\theta} = \text{block}-\text{diag}[\hat{\boldsymbol{\theta}}_1 \quad \hat{\boldsymbol{\theta}}_2 \quad \hat{\boldsymbol{\theta}}_3] \in \mathbb{R}^{\boldsymbol{3n\times 3}}$ is the matrix of weighting vectors for the three axis for which the update rule is designed as follows:

$$\dot{\hat{\boldsymbol{\theta}}} = \boldsymbol{\gamma}^{-1}\boldsymbol{\varphi}(\boldsymbol{X}_e)\hat{\boldsymbol{s}}^{\boldsymbol{T}} \quad (18)$$

$\boldsymbol{\gamma} = \text{dag}[\gamma_1 \quad \gamma_2 \quad \gamma_3]$ with $\gamma_i > 0 \in \mathbb{R}$ being the learning rate for the ith axis. The variable $\hat{\boldsymbol{s}} \in \mathbb{R}^{\boldsymbol{3}}$ is the filtered error function calculated using the estimated state variables as follows:

$$\hat{\boldsymbol{s}} = \dot{\hat{\boldsymbol{e}}} + \boldsymbol{\Gamma}\hat{\boldsymbol{e}} \quad (19)$$

where $\hat{e}^T = [\hat{e}_1 \quad \hat{e}_2 \quad \hat{e}_3]$ is the approximate tracking error vector, with $\hat{e}_1 = x_m - \hat{x}$, $\hat{e}_2 = y_m - \hat{y}$ and $\hat{e}_1 = z_m - \hat{z}$, and $\Gamma = \Gamma^T > 0 \in \mathbb{R}^{3\times 3}$ is chosen so that $\lim_{t\to\infty} \hat{\boldsymbol{e}} = 0$.

The difference between the FNN's output and the actual function being approximated is given by:

$$\hat{\boldsymbol{f}}(\boldsymbol{X}_e|\hat{\boldsymbol{\theta}}) - \boldsymbol{f}(\boldsymbol{q},\dot{\boldsymbol{q}}) = \tilde{\boldsymbol{\theta}}^{\boldsymbol{T}}\boldsymbol{\varphi}(\boldsymbol{X}_e) - \boldsymbol{\varepsilon}(\boldsymbol{X}_e) \quad (20)$$

where $\tilde{\boldsymbol{\theta}}$ represents the error on the approximated weight matrix, and the vector $\boldsymbol{\varepsilon}(\boldsymbol{X}_e) = [\varepsilon_1(\boldsymbol{X}_{e,1}) \quad \varepsilon_2(\boldsymbol{X}_{e,2}) \quad \varepsilon_3(\boldsymbol{X}_{e,3})]^{\boldsymbol{T}}$ represents the FNN's approximation error.

Assumption: There exist an unknown constant $\varepsilon_{ei,max} > 0$ such that the error $\varepsilon_i(\boldsymbol{X}_{e,i})$, for $1 \le i \le 3$, is bounded over the compact set $\Delta \in \mathbb{R}^6$, i.e. $\max_{X_{e,i}\in\mathbb{R}^6} |\varepsilon_i(\boldsymbol{X}_{e,i})| \le \varepsilon_{i,max}$.

To generate the actuation force for the 3-axis MEMS gyroscope, the control law is designed as follows:

$$\boldsymbol{u}(t) = \hat{\boldsymbol{f}}(\boldsymbol{X}_e|\hat{\boldsymbol{\theta}}) + \ddot{\boldsymbol{q}}_{\boldsymbol{m}} + \boldsymbol{\Gamma}\dot{\hat{\boldsymbol{e}}} + \hat{\boldsymbol{\eta}}(\boldsymbol{t})\boldsymbol{T}(\hat{\boldsymbol{s}}) + \boldsymbol{KE}(\hat{\boldsymbol{s}}) \quad (21)$$

It uses states $\hat{\boldsymbol{X}}$ estimated by the high-gain state observer given by Eq. (7) and the vector function $\hat{\boldsymbol{f}}(\boldsymbol{X}_e|\hat{\boldsymbol{\theta}})$ provided by the FNN's output. The constant matrix $\boldsymbol{K} = \boldsymbol{diag}[K_1 \quad K_2 \quad K_3]$ is a positive definite design parameter to be selected. The control law uses two nonlinear functions, $\boldsymbol{T}(\hat{\boldsymbol{s}}) = [T_1(\hat{s}_1) \quad T_2(\hat{s}_2) \quad T_3(\hat{s}_3)]^T$ and $\boldsymbol{E}(\hat{\boldsymbol{s}}) = [T_1(\hat{s}_1) \quad T_2(\hat{s}_2) \quad T_3(\hat{s}_3)]^T$, where $T_i(\hat{s}_i) = (\exp(4\hat{s}_i) - 1)/(\exp(4\hat{s}_i) + 1)$ and $E_i(\hat{s}_i) = \hat{s}_i/(\exp(\hat{s}_i) + 1)$, respectively, for $1 \le i \le 3$ [13]. The dynamic parameter $\hat{\boldsymbol{\eta}}(\boldsymbol{t}) \in \mathbb{R}^{\boldsymbol{3\times 3}}$ is expressed as follows:

$$\hat{\boldsymbol{\eta}}(\boldsymbol{t}) = \boldsymbol{\alpha}(\boldsymbol{t}) + \boldsymbol{\beta}(\boldsymbol{t}) \quad (22)$$

where $\boldsymbol{\beta}(\boldsymbol{t}) = \text{diag}[\rho|\hat{\varepsilon}_1| \quad \rho|\hat{\varepsilon}_2| \quad \rho|\hat{\varepsilon}_3|]$, $\rho > 0$, with the parameter $\hat{\varepsilon}_i \in \mathbb{R}$ being an estimation of the ith FNN's output approximation error ε_i upper bound and $\boldsymbol{\alpha}(t) = \text{diag}[\hat{\alpha}_1 \quad \hat{\alpha}_2 \quad \hat{\alpha}_3]$ is an estimation of the external disturbance's upper bound. The update rule for vector $\hat{\boldsymbol{\varepsilon}} = [\hat{\varepsilon}_1 \quad \hat{\varepsilon}_2 \quad \hat{\varepsilon}_3]^T$ is given as follows:

$$\hat{\boldsymbol{\varepsilon}} = \boldsymbol{\zeta}_{\boldsymbol{\varepsilon}}^{-1}\hat{\boldsymbol{s}} \quad (23)$$

where $\boldsymbol{\zeta}_{\boldsymbol{\varepsilon}} = \text{diag}[\zeta_{\varepsilon,1} \quad \zeta_{\varepsilon,2} \quad \zeta_{\varepsilon,3}]$ is a matrix of learning rate with $\boldsymbol{\zeta}_{\boldsymbol{\varepsilon},\boldsymbol{i}} \in \mathbb{R}^+$ for $1 \le i \le 3$.

ISSN (Print) : 2320 – 3765
ISSN (Online): 2278 – 8875

International Journal of Advanced Research in Electrical, Electronics and Instrumentation Engineering

(A High Impact Factor, Monthly, Peer Reviewed Journal)

Website: www.ijareeie.com

Vol. 8, Issue 8, August 2019

The dynamic parameter $\alpha(t) \in \mathbb{R}^{3\times 3}$ is computed using an adaptive law given as follows:

$$\dot{\hat{\boldsymbol{\alpha}}}(t) = \boldsymbol{\zeta}_\alpha^{-1}\hat{\boldsymbol{s}}^* \tag{24}$$

where $\hat{\boldsymbol{s}}^* = \text{diag}[\hat{s}_1 \quad \hat{s}_2 \quad \hat{s}_3]$ and the learning rate matrix is $\boldsymbol{\zeta}_\alpha = \text{diag}[\zeta_{\alpha,1} \quad \zeta_{\alpha,2} \quad \zeta_{\alpha,3}]$ with $\boldsymbol{\zeta}_{\alpha,i} \in \mathbb{R}^+$ for $1 \le i \le 3$.

In order to check the closed to system stability when the nonlinear control law given by Eq. (21) is applied to the 3-axis MEMS gyroscope, let us use the following candidate Lyapunov's function:

$$V = \frac{1}{2}\boldsymbol{s}^T\boldsymbol{s} + \frac{1}{2}\text{tr}\left[\tilde{\theta}^T\gamma\tilde{\theta}\right] + \frac{1}{2}\text{tr}[\tilde{\alpha}^T\zeta_\alpha\tilde{\alpha}] + \frac{1}{2}\tilde{\boldsymbol{\varepsilon}}^T\boldsymbol{\zeta}_\varepsilon\tilde{\boldsymbol{\varepsilon}} \tag{25}$$

where

$$\begin{cases} \tilde{\boldsymbol{\theta}} = \hat{\boldsymbol{\theta}} - \boldsymbol{\theta}^* \\ \tilde{\boldsymbol{\alpha}} = \hat{\boldsymbol{\alpha}} - \boldsymbol{\alpha} \\ \tilde{\boldsymbol{\varepsilon}} = \hat{\boldsymbol{\varepsilon}} - \boldsymbol{\varepsilon} \end{cases} \tag{26}$$

The matrix $\tilde{\boldsymbol{\theta}} \in \mathbb{R}^{3n\times 3}$ represents the error on the approximated weight matrix $\hat{\boldsymbol{\theta}}$, with $\boldsymbol{\theta}^* \in \mathbb{R}^{3m\times 3}$; $\tilde{\boldsymbol{\alpha}}$ is the error on the approximate matrix $\hat{\boldsymbol{\alpha}}$; $\tilde{\boldsymbol{\varepsilon}}$ is the approximation error for $\hat{\boldsymbol{\varepsilon}}$.
The first order derivative of the Lyapunov's function is obtained as follows:

$$\dot{V} = \boldsymbol{s}^T\dot{\boldsymbol{s}} + \text{tr}\left[\tilde{\theta}^T\gamma\dot{\hat{\theta}}\right] + \text{tr}\left[\tilde{\alpha}^T\zeta_\alpha\dot{\hat{\alpha}}\right] + \tilde{\boldsymbol{\varepsilon}}^T\boldsymbol{\zeta}_\varepsilon\dot{\hat{\boldsymbol{\varepsilon}}} \tag{27}$$

With the exact state variables, the filtered error vector function is expressed as follows:

$$\boldsymbol{s} = \dot{\boldsymbol{e}} + \boldsymbol{\Gamma}\mathbf{e} \tag{28}$$

Deriving $\boldsymbol{s}$ with respect to time, and using $\ddot{\boldsymbol{e}} = \ddot{\boldsymbol{q}}_{\boldsymbol{m}} - \ddot{\boldsymbol{q}}$ and Eqs. (13), (20) and (21) yields:

$$\dot{\boldsymbol{s}} = -\left[\tilde{\boldsymbol{\theta}}^T\boldsymbol{\varphi}(\boldsymbol{X}_e) - \boldsymbol{\varepsilon}(\boldsymbol{X}_e)\right] + \boldsymbol{\Gamma}\left(\dot{\boldsymbol{e}} - \dot{\hat{\boldsymbol{e}}}\right) - \hat{\boldsymbol{\eta}}(\boldsymbol{t})\boldsymbol{T}(\hat{\boldsymbol{s}}) - \boldsymbol{K}\boldsymbol{E}(\hat{\boldsymbol{s}}) + \boldsymbol{d}(\boldsymbol{t}) \tag{29}$$

Applying Eqs. (26) and (29) in Eq. (27) yields:

$$\begin{aligned} \dot{V} &= \boldsymbol{s}^T\left\{-\left[\tilde{\boldsymbol{\theta}}^T\boldsymbol{\varphi}(\boldsymbol{X}_e) - \boldsymbol{\varepsilon}(\boldsymbol{X}_e)\right] + \boldsymbol{\Gamma}\left(\dot{\boldsymbol{e}} - \dot{\hat{\boldsymbol{e}}}\right) - \hat{\boldsymbol{\eta}}(\boldsymbol{t})\boldsymbol{T}(\hat{\boldsymbol{s}}) - \boldsymbol{K}\boldsymbol{E}(\hat{\boldsymbol{s}}) - \boldsymbol{d}(\boldsymbol{t})\right\} + \text{tr}\left[\tilde{\boldsymbol{\theta}}^T\boldsymbol{\gamma}\dot{\hat{\boldsymbol{\theta}}}\right] + \text{tr}\left[\tilde{\boldsymbol{\alpha}}^T\boldsymbol{\zeta}_\alpha\dot{\hat{\boldsymbol{\alpha}}}\right] + \tilde{\boldsymbol{\varepsilon}}^T\boldsymbol{\zeta}_\varepsilon\dot{\hat{\boldsymbol{\varepsilon}}} \\ &= \textbf{tr}\left[\tilde{\boldsymbol{\theta}}^T\left(\boldsymbol{\gamma}\dot{\hat{\boldsymbol{\theta}}} - \boldsymbol{\varphi}(\boldsymbol{X}_e)\boldsymbol{s}^T\right)\right] + \boldsymbol{s}^T\,\boldsymbol{\varepsilon}(\boldsymbol{X}_e) + \boldsymbol{s}^T\boldsymbol{d}(\boldsymbol{t}) - \boldsymbol{s}^T\hat{\boldsymbol{\eta}}(\boldsymbol{t})\boldsymbol{T}(\hat{\boldsymbol{s}}) - \boldsymbol{s}^T\boldsymbol{K}\boldsymbol{E}(\hat{\boldsymbol{s}}) + \text{tr}\left[\tilde{\boldsymbol{\alpha}}^T\boldsymbol{\zeta}_\alpha\dot{\hat{\boldsymbol{\alpha}}}\right] + \tilde{\boldsymbol{\varepsilon}}^T\boldsymbol{\zeta}_\varepsilon\dot{\hat{\boldsymbol{\varepsilon}}} \end{aligned} \tag{30}$$

Let us now use the update rules given by Eqs. (18), (23) and (24) and the identities given by Eq. (26), while considering the convergence property of the high-gain state observer (i.e. $\hat{\boldsymbol{s}} \to \boldsymbol{s}$) to obtain:

$$\begin{aligned} \dot{V} &= \textbf{tr}\left[\tilde{\boldsymbol{\theta}}^T\boldsymbol{\varphi}(\boldsymbol{X}_e)(\hat{\boldsymbol{s}}^T - \boldsymbol{s}^T)\right] + \boldsymbol{s}^T\,(\hat{\boldsymbol{\varepsilon}} - \tilde{\boldsymbol{\varepsilon}}) + \boldsymbol{s}^T\boldsymbol{d}(\boldsymbol{t}) - \boldsymbol{s}^T\hat{\boldsymbol{\eta}}(\boldsymbol{t})\boldsymbol{T}(\hat{\boldsymbol{s}}) - \boldsymbol{s}^T\boldsymbol{K}\boldsymbol{E}(\hat{\boldsymbol{s}}) + \text{tr}\left[\tilde{\boldsymbol{\alpha}}^T\boldsymbol{\zeta}_\alpha\dot{\hat{\boldsymbol{\alpha}}}\right] + \tilde{\boldsymbol{\varepsilon}}^T\boldsymbol{\zeta}_\varepsilon\dot{\hat{\boldsymbol{\varepsilon}}} \\ &\cong \boldsymbol{s}^T(\hat{\boldsymbol{\varepsilon}} - \tilde{\boldsymbol{\varepsilon}}) + \boldsymbol{s}^T\boldsymbol{d}(\boldsymbol{t}) - \boldsymbol{s}^T\hat{\boldsymbol{\eta}}(\boldsymbol{t})\boldsymbol{T}(\hat{\boldsymbol{s}}) - \boldsymbol{s}^T\boldsymbol{K}\boldsymbol{E}(\hat{\boldsymbol{s}}) + \text{tr}\left[\tilde{\boldsymbol{\alpha}}^T\boldsymbol{\zeta}_\alpha\dot{\hat{\boldsymbol{\alpha}}}\right] + \tilde{\boldsymbol{\varepsilon}}^T\boldsymbol{\zeta}_\varepsilon\dot{\hat{\boldsymbol{\varepsilon}}} \\ &= \boldsymbol{s}^T\left(\boldsymbol{\zeta}_\varepsilon\dot{\hat{\boldsymbol{\varepsilon}}} - \boldsymbol{s}\right) + \boldsymbol{s}^T\boldsymbol{d}(\boldsymbol{t}) - \boldsymbol{s}^T\hat{\boldsymbol{\eta}}(\boldsymbol{t})\boldsymbol{T}(\hat{\boldsymbol{s}}) - \boldsymbol{s}^T\boldsymbol{K}\boldsymbol{E}(\hat{\boldsymbol{s}}) + \text{tr}\left[\tilde{\boldsymbol{\alpha}}^T\boldsymbol{\zeta}_\alpha\dot{\hat{\boldsymbol{\alpha}}}\right] + \boldsymbol{s}^T\hat{\boldsymbol{\varepsilon}} \\ &= \tilde{\boldsymbol{\varepsilon}}^T(\hat{\boldsymbol{s}} - \boldsymbol{s}) + \boldsymbol{s}^T\boldsymbol{d}(\boldsymbol{t}) - \boldsymbol{s}^T\hat{\boldsymbol{\eta}}(\boldsymbol{t})\boldsymbol{T}(\hat{\boldsymbol{s}}) - \boldsymbol{s}^T\boldsymbol{K}\boldsymbol{E}(\hat{\boldsymbol{s}}) + \text{tr}\left[\tilde{\boldsymbol{\alpha}}^T\boldsymbol{\zeta}_\alpha\dot{\hat{\boldsymbol{\alpha}}}\right] + \boldsymbol{s}^T\hat{\boldsymbol{\varepsilon}} \\ &\cong \boldsymbol{s}^T\boldsymbol{d}(\boldsymbol{t}) - \boldsymbol{s}^T\hat{\boldsymbol{\eta}}(\boldsymbol{t})\boldsymbol{T}(\hat{\boldsymbol{s}}) - \boldsymbol{s}^T\boldsymbol{K}\boldsymbol{E}(\hat{\boldsymbol{s}}) + \text{tr}\left[\tilde{\boldsymbol{\alpha}}^T\boldsymbol{\zeta}_\alpha\dot{\hat{\boldsymbol{\alpha}}}\right] + \boldsymbol{s}^T\hat{\boldsymbol{\varepsilon}} \end{aligned} \tag{31}$$

During the worst situation caused by external disturbances or varying system parameters, the filtered error function $\tilde{\boldsymbol{s}}$ diverges from the origin such that $T_i(\hat{s}_i) = (\exp(4\hat{s}_i) - 1)/(\exp(4\hat{s}_i) + 1) \cong 1$. Hence, Eq. (31) where the identity given by Eq. (22) is used, becomes:

ISSN (Print) : 2320 – 3765
ISSN (Online): 2278 – 8875

International Journal of Advanced Research in Electrical, Electronics and Instrumentation Engineering

(A High Impact Factor, Monthly, Peer Reviewed Journal)

Website: www.ijareeie.com

Vol. 8, Issue 8, August 2019

$$\dot{V} \cong \boldsymbol{s}^T\boldsymbol{d}(\boldsymbol{t}) - \boldsymbol{s}^T\widehat{\boldsymbol{\eta}}(\boldsymbol{t})\boldsymbol{I}_3 - \boldsymbol{s}^T\boldsymbol{K}\boldsymbol{E}(\hat{\boldsymbol{s}}) + \mathrm{tr}\big[\widetilde{\boldsymbol{\alpha}}^T\boldsymbol{\zeta}_{\alpha}\dot{\widehat{\boldsymbol{\alpha}}}\big] + \boldsymbol{s}^T\hat{\boldsymbol{\varepsilon}}$$
$$= \boldsymbol{s}^T\boldsymbol{d}(\boldsymbol{t}) - \boldsymbol{s}^T[\boldsymbol{\alpha}(\boldsymbol{t}) + \boldsymbol{\beta}(\boldsymbol{t})\,]\boldsymbol{I}_3 - \textstyle\sum_{i=1}^{3}\boldsymbol{K}_i\frac{\hat{s}_i s_i}{\exp(\hat{s}_i)+1} + \mathrm{tr}\big[\widetilde{\boldsymbol{\alpha}}^T\boldsymbol{\zeta}_{\alpha}\dot{\widehat{\boldsymbol{\alpha}}}\big] + \boldsymbol{s}^T\hat{\boldsymbol{\varepsilon}} - \boldsymbol{s}^T\boldsymbol{\alpha}\boldsymbol{I}_3 + \boldsymbol{s}^T\boldsymbol{\alpha}\boldsymbol{I}_3 \tag{32}$$

where $\boldsymbol{I}_3 \in \mathbb{R}^{3\times3}$ is an identity matrix. Considering the convergence property of the observer and using the expression of $\widetilde{\boldsymbol{\alpha}}$ given by Eq. (26) and the update rule given by Eq. (24) yields:

$$\dot{V} = \boldsymbol{s}^T\boldsymbol{d}(\boldsymbol{t}) - \boldsymbol{s}^T[-\widehat{\boldsymbol{\alpha}} + \boldsymbol{\alpha}(\boldsymbol{t})\,]\boldsymbol{I}_3 - \textstyle\sum_{i=1}^{3}\boldsymbol{K}_i\frac{s_i^2}{\exp(\hat{s}_i)+1} + \mathrm{tr}\big[\widetilde{\boldsymbol{\alpha}}^T\boldsymbol{\zeta}_{\alpha}\dot{\widehat{\boldsymbol{\alpha}}}\big] + \boldsymbol{s}^T\hat{\boldsymbol{\varepsilon}} - \boldsymbol{s}^T\boldsymbol{\alpha}_1\boldsymbol{I}_3 - \boldsymbol{s}^T\boldsymbol{\beta}\boldsymbol{I}_3$$
$$= \boldsymbol{s}^T\boldsymbol{d}(\boldsymbol{t}) + \mathbf{tr}\big[\widehat{\boldsymbol{\alpha}}^T\big(\boldsymbol{\zeta}_{\alpha}\dot{\widehat{\boldsymbol{\alpha}}} - \boldsymbol{I}_3\boldsymbol{s}^T\big)\big] - \textstyle\sum_{i=1}^{3}\boldsymbol{K}_i\frac{s_i^2}{\exp(\hat{s}_i)+1} + \boldsymbol{s}^T\hat{\boldsymbol{\varepsilon}} - \boldsymbol{s}^T\boldsymbol{\alpha}_1\boldsymbol{I}_3 - \boldsymbol{s}^T\boldsymbol{\beta}\boldsymbol{I}_3$$
$$= \boldsymbol{s}^T\boldsymbol{d}(\boldsymbol{t}) + \mathbf{tr}[\widehat{\boldsymbol{\alpha}}^T(\hat{\boldsymbol{s}}^* - \boldsymbol{s}^*)] - \textstyle\sum_{i=1}^{3}\boldsymbol{K}_i\frac{s_i^2}{\exp(\hat{s}_i)+1} + \boldsymbol{s}^T\hat{\boldsymbol{\varepsilon}} - \boldsymbol{s}^T\boldsymbol{\alpha}_1\boldsymbol{I}_3 - \boldsymbol{s}^T\boldsymbol{\beta}\boldsymbol{I}_3 \tag{33}$$
$$\cong \boldsymbol{s}^T\boldsymbol{d}(\boldsymbol{t}) - \textstyle\sum_{i=1}^{3}\boldsymbol{K}_i\frac{s_i^2}{\exp(\hat{s}_i)+1} + \boldsymbol{s}^T\hat{\boldsymbol{\varepsilon}} - \boldsymbol{s}^T\boldsymbol{\alpha}_1\boldsymbol{I}_3 - \boldsymbol{s}^T\boldsymbol{\beta}\boldsymbol{I}_3$$
$$\leq \boldsymbol{s}^T\boldsymbol{d}(\boldsymbol{t}) - \textstyle\sum_{i=1}^{3}\boldsymbol{K}_i\frac{s_i^2}{\exp(\hat{s}_i)+1} + \|\boldsymbol{s}\|(\|\boldsymbol{d}\| - \|\boldsymbol{\alpha}\|) + \|\boldsymbol{s}\|(\|\hat{\boldsymbol{\varepsilon}}\| - \|\boldsymbol{\beta}\|)$$

Knowing that $\boldsymbol{\beta} = \mathrm{diag}[\rho|\hat{\varepsilon}_1| \quad \rho|\hat{\varepsilon}_2| \quad \rho|\hat{\varepsilon}_3|]$, $\rho > 0$ such that $\|\boldsymbol{\beta}\| = \boldsymbol{\rho}\|\hat{\boldsymbol{\varepsilon}}\|$ Eq. (33) becomes:

$$\dot{V} \leq \boldsymbol{s}^T\boldsymbol{d}(\boldsymbol{t}) - \textstyle\sum_{i=1}^{3}K_i\frac{s_i^2}{\exp(\hat{s}_i)+1} + \|\boldsymbol{s}\|(\|\boldsymbol{d}\| - \|\boldsymbol{\alpha}\|) + \|\boldsymbol{s}\|\left(\frac{1}{\rho} - \mathbf{1}\right)\|\boldsymbol{\beta}\| \tag{34}$$

Considering that $\|\boldsymbol{\alpha}\| \gg \|\boldsymbol{d}\|$ (it is worth noting that $\boldsymbol{\alpha}$ is used only for analytic purpose but it is not needed for the controller's implementation), and selecting $\rho > 1$, with $K_i \in \mathbb{R}^+$, we have $\dot{V} \leq 0$. Thus, with the proposed control law, with its dynamic parameters and state observer, the control objective is achieved as the closed-loop system is asymptotically stable despite uncertain system parameters, FNN approximation errors and external disturbances.

IV. SIMULATION AND DISCUSSION

Let us illustrate the efficiency of the designed control scheme for the 3-axis MEMS gyroscope by presenting simulation results obtained using MATLAB/SIMULINK. The control objective consists in forcing the position vector $\boldsymbol{q}$ to track the reference trajectory $\boldsymbol{q_m} = [x_m \quad y_m \quad z_m]^T$ where $x_m = \sin(6.71t)$, $y_m = 1.2\sin(5.11t)$ and $z_m = 1.5\sin(4.17t)$. The parameters of the simulated 3-axis MEMS gyroscope are as follows [4]: $m = 0.57 \times 10^{-8}kg$, $q_0 = 1\mu m$, $\omega_0 = 3kHz$, $d_{xx} = 0.429 \times 10^{-6}Ns/m$, $d_{yy} = 0.687 \times 10^{-6}Ns/m$, $d_{zz} = 0.895 \times 10^{-6}Ns/m$, $d_{xy} = 0.0429 \times 10^{-6}Ns/m$, $d_{xz} = 0.0687 \times 10^{-6}Ns/m$, $d_{yz} = 0.0895 \times 10^{-6}Ns/m$, $k_{xx} = 80.98\ N/m$, $k_{yy} = 71.62\ N/m$, $k_{zz} = 60.97\ N/m$, $k_{xy} = 5\ N/m$, $k_{xz} = 6\ N/m$, $k_{yz} = 7\ N/m$. We assume that the unknown angular velocities are $\Omega_x = 3\ rad/s$, $\Omega_y = 2rad/s$ and $\Omega_z = 5\frac{rad}{s}$.

The parameter settings for the high-gain observer are selected, for $1 \leq i \leq 3$, as $L_i = \left[\frac{18}{\sigma(t)} \quad \frac{9}{\sigma(t)}\right]^T$ where $\sigma(t)$ is given by Eq. (8). For the FNN used to approximate the unknown dynamics (as the MEMS gyroscope parameters are not used for the controller's implementation) we use five fuzzy rules for each axis. The following membership function is implemented for each axis:

$$\mu_{A_l^j} = \exp\left[-\frac{\left(X_{ei,l} + 1.5 - (j-1)0.5\right)^2}{10^2}\right] \tag{35}$$

where $X_{ei,l} = [\hat{q}_i \quad \dot{\hat{q}}_i]^T$, $i = 1, 2, 3$, $1 \leq j \leq 5$ and $l = 1, 2$. The learning rates for each axis's weighting vector is selected as $\gamma_i = 15$ for $i = 1, 2, 3$. The learning rate for the dynamic parameters $\hat{\boldsymbol{\varepsilon}}(t)$ and $\boldsymbol{\alpha}(t)$ are selected as $\zeta_{\varepsilon,i} = 0.5$ and $\zeta_{\alpha,i} = 1800$ for $i = 1, 2, 3$, respectively. For the filtered error function, the entries of the diagonal matrix $\Gamma \in \mathbb{R}^3$ are selected as 50 on the diagonal. For the dynamic parameter $\boldsymbol{\beta}(t)$ we select $\rho = 450$. The controller's parameter $\boldsymbol{K} = \boldsymbol{K}^T \in \mathbb{R}^{3\times3}$ elements are selected as $K_i = 25$, for $1 \leq i \leq 3$. The external disturbance is $d(t) = [10\sin(6t) \quad 10\cos(5t) \quad 10\cos(4t)]^T$.

ISSN (Print) : 2320 – 3765
ISSN (Online): 2278 – 8875

International Journal of Advanced Research in Electrical, Electronics and Instrumentation Engineering

(A High Impact Factor, Monthly, Peer Reviewed Journal)

Website: www.ijareeie.com

Vol. 8, Issue 8, August 2019

For this simulation, the initial system's state vector is selected as $\boldsymbol{X_0} = [0.5\ 0\ 0.5\ 0\ 1\ 0]$. Figure 1 shows the three axis positions x, y and z tracking their given references x_m, y_m and z_m.

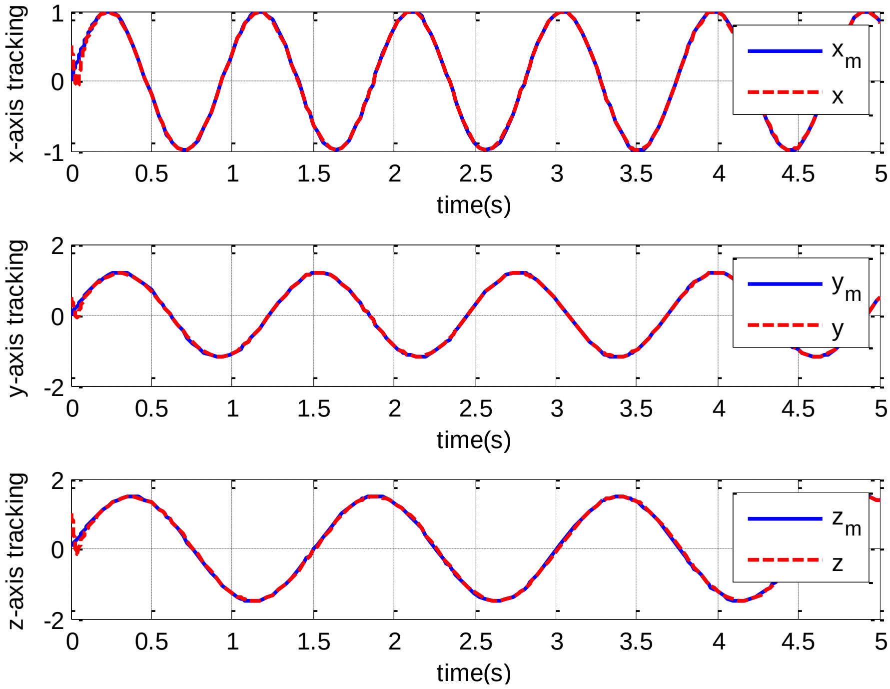

Fig. 1 Position tracking on the x, y and z axis

One can observe in Fig. 1 that, starting from different initial conditions, the MEMS gyroscope states converge and remain very close to the desired states x_m, y_m and z_m. This is achieved after a very short transient phase (nearly at $t = 0.1s$). Let us remind that this very good tracking accuracy is obtained using a state observer, which provides an accurate estimation of the unmeasured states $\dot{x}$, $\dot{y}$ and $\dot{z}$. Figure 2 depicts states $\dot{x}$, $\dot{y}$ and $\dot{z}$ with their estimated values $\hat{\dot{x}}$, $\hat{\dot{y}}$ and $\hat{\dot{z}}$ obtained using the high-gain state observer given by Eq. (7).

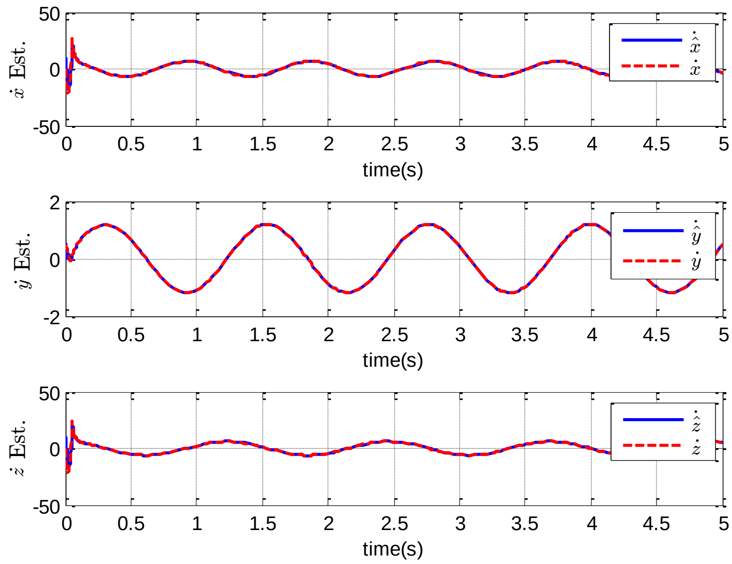

Fig. 2 State estimation by the high-gain state observer

ISSN (Print) : 2320 – 3765
ISSN (Online): 2278 – 8875

International Journal of Advanced Research in Electrical, Electronics and Instrumentation Engineering

(A High Impact Factor, Monthly, Peer Reviewed Journal)

Website: www.ijareeie.com

Vol. 8, Issue 8, August 2019

The good tracking accuracy depicted in Fig.1 is also obtained thanks to the control action generated using the proposed control law. Figure 3 shows control forces on the three axis.

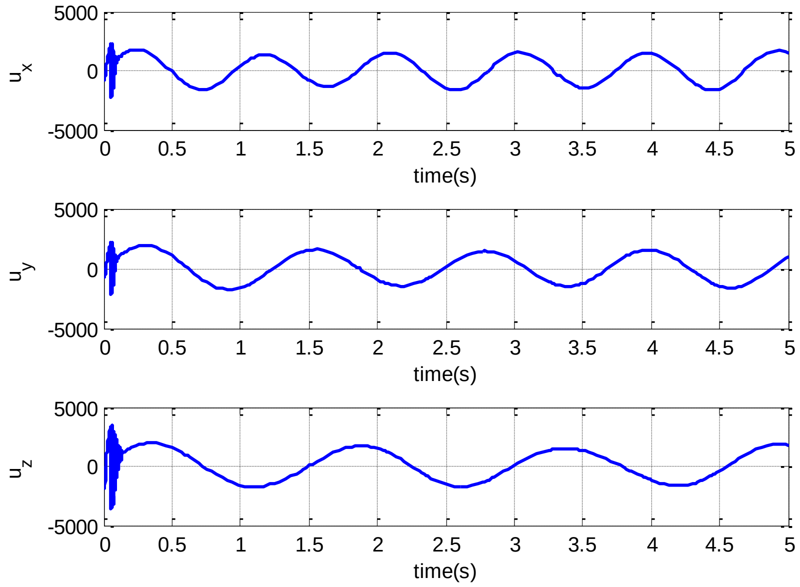

Fig .3 Throughput of sending bits Vs Maximal simulation jitter

V.CONCLUSION

This paper has presented a nonlinear control scheme for a 3-axis MEMS gyroscope subject to external disturbances and uncertain dynamics or parameters. The control schemes exploits the universal approximation theorem related to FNN to approximate the unknown dynamics to be used for the controller's implementation without requiring the knowledge of the MEMS parameters. As for this study full state measurement was considered unavailable, a model-free high-gain state observed has been used, which is able to provide an accurate estimation of the state vector. Simulation results have shown that a very good tracking accuracy is obtained on the three axis despite external disturbance and FNN approximation errors.

REFERENCES

[1] W. Li and P. Liu, "Adaptive tracking control of an MEMS gyroscope with H-infinity performance," *J Control Theory Appl,* vol. 9, no. 2, pp. 237-243, 2011.

[2] D. Nauck and R. Kruse, "Neuro-fuzzy systems for function approximation," *Fuzzy Sets and Systems,* vol. 101, pp. 261-271, 1999.

[3] C. Lin and C. Lee, "Neural-network-based fuzzy logic control and decision system," *IEEE Transactions on Computers,* vol. 40, no. 12, pp. 1320-1336, 1991.

[4] J. Fei and M. Xin, "An adaptive fuzzy sliding mode controller for MEMS triaxial gyroscope with angular velocity estimation," *Nonlinear Dyn,* 2012.

[5] G. Rigatos, G. Zhu, H. Yousef and A. Boulkroune, "Flatness-based adaptive fuzzy control of electrostatically actuated MEMS using output feedback," *Fuzzy Sets and Systems,* vol. 290, pp. 138-157, 2016.

[6] X. Liang, S. Li and J. Fei, "Adaptive Fuzzy Global Fast Terminal Sliding Mode Control for Microgyroscope System," *IEEE Access,* vol. 4, pp. 9681-9688, 2016.

[7] D. Lei, T. Wang, D. Cao and J. Fei, "Adaptive Dynamic Surface Control of MEMS Gyroscope Sensor Using Fuzzy Compensator," *IEEE Acces,* vol. 4, pp. 4148-4154, 2006.

[8] A. Ghanbari and M. Moghanni-Bavil-Olyaei, "Adaptive fuzzy terminal sliding-mode control of MEMS z-axis gyroscope with extended Kalman filter observer," *Systems Science & Control Engineering: An Open Access Journal,* vol. 2, pp. 183-191, 2014.

[9] Y. Chu, J. Fei and S. Hou, "Adaptive Neural Backstepping PID Global Sliding Mode Fuzzy Control of MEMS Gyroscope," *IEEE Access,* 2019.

ISSN (Print) : 2320 – 3765
ISSN (Online): 2278 – 8875

International Journal of Advanced Research in Electrical, Electronics and Instrumentation Engineering

(A High Impact Factor, Monthly, Peer Reviewed Journal)

Website: www.ijareeie.com

Vol. 8, Issue 8, August 2019

[10] C. Lu and F. Juntao, “Backstepping control of MEMS gyroscope using adaptive neural observer,” *Int. J. Mach. Learn. & Cyber.*, 2016.

[11] R. P. Leland, “Adaptive Control of a MEMS Gyroscope Using Lyapunov Methods,” *IEEE TRANSACTIONS ON CONTROL SYSTEMS TECHNOLOGY,* vol. 14, no. 2, pp. 278-283, 206.

[12] Liu, J., Wang, X., Advanced Sliding Mode Control for Mechanical Systems, Beijing: Tsinghua University Press, 2011.

[13] B. Mushage, J. Chedjou and K. Kyamakya, “Fuzzy neural network and observer-based fault-tolerant adaptive nonlinear control of uncertain 5-DOF upper-limb exoskeleton robot for passive rehabilitation,” *Nonlinear Dyn,* vol. 87, pp. 2021-2037, 2017.

[14] M. Armenise, C. Ciminelli, F. Dell'Olio and V. Passaro, Advances in Gyroscope Technologies, Berlin Heidelberg: Springer-Verlag, 2011.

[15] M. Saif, B. Ebrahimi and M. Vali, “A second order sliding mode strategy for fault detection and fault-tolerant control of a MEMS optical switch,” *Mechatronics,* vol. 22, pp. 696-705, 2012.

[16] Q. Zheng, L. Dong, D. H. Lee and Z. Gao, “Active Disturbance Rejection Control for MEMS Gyroscopes,” *IEEE TRANSACTIONS ON CONTROL SYSTEMS TECHNOLOGY,* vol. 17, no. 6, pp. 1432-1438, 2009.

[17] D. Wu, D. Cao, T. Wang, Y. Fang and J. Fei, “Adaptive Neural LMI-Based H-Infinity Control for MEMS Gyroscope,” *IEEE Access,* vol. 4, pp. 6624-6630, 2016.

[18] M. Rahmani, “MEMS gyroscope control using a novel compound robust control,” *ISA Transactions,* 2017.

[19] R. Zhang, T. Shao, W. Zhao, A. Li and B. Xu, “Sliding mode control of MEMS gyroscopes using composite learning,” *Neurocomputing,* vol. 275, pp. 2555-2564, 2018.

[20] K. Veluvolu, M. Defoort and Y. Soh, “High-gain observer with sliding mode for nonlinear state estimation and fault reconstruction,” *J. Frankl. Inst.,* vol. 351, p. 1995–2014, 2014.

[21] K. Veluvolu, M. Kim and D. Lee, “Nonlinear sliding mode high-gain observers for fault estimation,” *Int. J. Syst. Sci.,* vol. 42, p. 1065–1074, 2011.

[22] B. Pratap and S. Purwar, “Sliding mode state observer for 2-DOF twin rotor MIMO system.,” in *2010 International Conference on Power. Control and Embedded Systems (ICPCES)* , Allahabad, 2010.

[23] K. Z. F. S. Y. Veluvolu, “Nonlinear sliding mode high-gain observers for fault detection,” in *2010 International Workshop on Variable Structure Systems*, Mexico City.

[24] K. S. Y. C. W. Veluvolu, “Robust observer with sliding mode estimation for nonlinear uncertain systems,” *IET Control Theory Appl. 1(5),* vol. 1, no. 5, p. 1533–1540, 2007.